Molecular Crystals and Liquid Crystals Science and Technology. Section A. Molecular Crystals and Liquid Crystals
Publication details, including instructions for authors and subscription information:
http://www.tandfonline.com/loi/gmcl19

FT Pulsed ESR/Electron Spin Transient Nutation Spectroscopy in the Study of Molecular Based Magnetism: Applications to High-Spin Polymers and Ferromagnetic Materials

Takeji Takui [a] , Kazunobu Sato [a] , Daisuke Shiomi [b] , Koichi Itoh [b] , Takashi Kaneko [c] , Eishun Tsuchida [c] & Hiroyuki Nishide [c]

[a] Department of Chemistry, Faculty of Science, Osaka City University, Sugimoto, Sumiyoshi-ku, Osaka, 558

[b] Department of Material Science, Faculty of Science, Osaka City University, Sugimoto, Sumiyoshi-ku, Osaka, 558

[c] Department of Applied Chemistry, Faculty of Science and Engineering, Waseda University, Okubo, Shinjuku-ku, Tokyo, 169, Japan

Version of record first published: 24 Sep 2006.

To cite this article: Takeji Takui , Kazunobu Sato , Daisuke Shiomi , Koichi Itoh , Takashi Kaneko , Eishun Tsuchida & Hiroyuki Nishide (1995): FT Pulsed ESR/Electron Spin Transient Nutation Spectroscopy in the Study of Molecular Based Magnetism: Applications to High-Spin Polymers and Ferromagnetic Materials, Molecular Crystals and Liquid Crystals Science and Technology. Section A. Molecular Crystals and Liquid Crystals, 271:1, 191-212

To link to this article: http://dx.doi.org/10.1080/10587259508034052

Mol. Cryst. Liq. Cryst., 1995, Vol. 271, pp. 191–212
Reprints available directly from the publisher
Photocopying permitted by license only

FT PULSED ESR/ELECTRON SPIN TRANSIENT NUTATION SPECTROSCOPY IN THE STUDY OF MOLECULAR BASED MAGNETISM: APPLICATIONS TO HIGH-SPIN POLYMERS AND FERROMAGNETIC MATERIALS

TAKEJI TAKUI,[1] KAZUNOBU SATO,[1] DAISUKE SHIOMI,[2] KOICHI ITOH,[2] TAKASHI KANEKO,[3] EISHUN TSUCHIDA,[3] and HIROYUKI NISHIDE[3]
[1]Department of Chemistry and [2]Department of Material Science, Faculty of Science, Osaka City University, Sugimoto, Sumiyoshi-ku, Osaka 558; [3]Department of Applied Chemistry, Faculty of Science and Engineering, Waseda University, Okubo, Shinjuku-ku, Tokyo 169, Japan

Abstract Recently, organic high-spin polymers and clusters have been emerging. With the increasing effective molecular spin quantum number S and molecular weight of the polymers, however, cw ESR spectroscopy manifests its inherent disadvantages in discriminating high spins from S=1/2 and in determining the S's for the complex mixture of various spin assemblages. An electron spin transient nutation method based on pulsed ESR spectroscopy has been for the first time applied to a quasi 1D high-spin polymer as one of the most complex amorphous spin assemblages, identifying that the polymer is comprised of high-spin assemblages with the S's greater than two. It can be concluded that electron spin transient nutation spectroscopy is a facile and useful method for the exclusive identification of S and ESR transitions even for the cases of apparently vanishing fine-structure splittings and for spin systems with residual fine-structure terms in the spin Hamiltonian. Fundamental bases for the transient nutation method are described, emphasizing inherent advantages in the nutation spectroscopy from the methodological viewpoint. The salient features of multiple-quantum nutations have been disclosed in this work.

INTRODUCTION

Pulse Fourier transform NMR spectroscopy has made traditional cw NMR obsolete during the past two decades, leading to a continuing and unprecedented expansion of NMR applications. Recently in ESR spectroscopy, pulsed FT-spectroscopic techniques continue to emerge[1–7] because of the advantages intrinsic to FT spectroscopy in many experimental aspects, emphasizing the capability of measuring transient properties of electron-nuclear spin systems, the adaptability to other pulsed spectroscopic techniques, and the inherent advantages of coherence-transfer based 2D time-domain spectroscopy. The methodology of quantum spin transient nutation to measure the spin Hamiltonian in terms of the rotating frame has been developed in NMR/NQR spectroscopy[8–14] and appeared in ESR spectroscopy at early times.[15–17] It was not until recently that nutation methods were introduced as pulsed

ESR spectroscopic techniques.[18,19] Isoya et al. have determined the effective spin quantum number S for the nickel impurity in synthetic diamond to be S=3/2 with non-vanishing fine-structure constants due to a distortion of the impurity site from tetrahedral symmetry.[18] Astashkin and Schweiger have demonstrated that an electron spin transient nutation method facilitates the identification of complex single-crystal ESR spectra from transition metal ions by exploiting the nutation frequency dependence of the allowed and forbidden transitions.[19]

The purposes of this work have been twofold. Firstly, the nutation method has been applied to inorganic high-spin systems in the powder state in order to demonstrate that electron spin transient nutation spectroscopy is capable of elaborating useful information on electronic and environmental structures of paramagnetic centers which cw ESR spectroscopy can not afford. This is the first attempt to apply the nutation method to non-oriented samples. Secondly, the nutation spectroscopy has been applied to organic solid-state magnetic polymers as one of the most complex spin systems, where robust intermolecular exchange interaction takes place. The results have shown the inherent potentiality of the nutation spectroscopy to identify effective molecular spin multiplicities of complicated spin assemblages in amorphous materials. Recently, organic molecular based magnetism [20,21] has been the focus of current topics in chemistry, physics, and their related fields in both pure and applied sciences.[22,23] For the second purpose, we adopt a quasi one-dimensional high-spin polymer as models for high Tc organic ferromagnets. With the increasing effective molecular spin quantum number S and molecular weight of π-conjugated organic high-spin or magnetic polymers, particularly polymers characterized by small spin-spin interactions, cw ESR spectroscopy reveals its

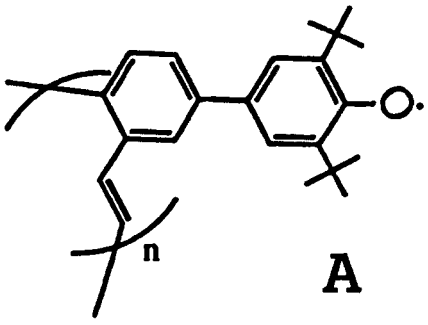

A

FIGURE 1 Quasi 1D magnetic polymer as models for quasi 1D organic ferrromagnets. The π-conjugated electron netwok is governed by topologically controlled spin polarization (through-bond approach).

inherent disadvantages in discriminating high spins from S=1/2 and determining the effective spin quantum numbers of high spins for the mixture of various spin assemblages. FT pulsed ESR spectroscopy has been applied to one of the first organic high-spin polymers A (see Figure 1)[24] in order to identify molecular spin multiplicities comprising the polymer in the solid state.

FUNDAMENTAL BASES FOR ELECTRON SPIN TRANSIENT NUTATION SPECTROSCOPY

Nutation Spectrum of Single Quantum Transitions

We describe the electron spin transient nutation of single quantum transitions first in terms of a classical vectorial picture for the motion of the spin magnetization and next in terms of a quantum mechanical approach. This is for the convenience of the readers who might not be familiar with nutation phenomena in magnetic resonance. Next we describe features of the transient nutation appearing in multiple quantum transitions. These features have been disclosed in the present work.

Electron spin transient nutation spectroscopy is based on electron spin resonance to measure the spin Hamiltonian in terms of the rotating frame.[4-6] The electron spin magnetization $\mathbf{M}_0$ in the presence of a static magnetic field $\mathbf{B}_0$ presseses at the corresponding nutation angle ϕ from the initial direction around the effective field $\mathbf{B}_{eff} = \mathbf{B}_0 + \mathbf{B}_1$ by applying the microwave field ($\mathbf{B}_1$) pulse with the width t_1 (see Figure 2). Then the magnetization $\mathbf{M}_0$ in thermal equilibrium undergoes free induction decay (FID) when the excitation pulse is turned off. The nutation is described in terms of the above classical vectorial picture for the motion of the magnetization as follows. The magnetization components M_x and M_y in the frame xyz rotating with a frequency ω are given as

$$M_x = M_0 \sin\phi/(1+x^2)^{1/2} \tag{1}$$

$$M_y = M_0 [2x/(1+x^2)] \sin^2[\phi/2] \tag{2}$$

$$\begin{aligned} M_m &= M_0 [1/(1+x^2)\{\sin^2\phi + x^2(1-\cos\phi)^2/(1+x^2)\}]^{1/2} \\ &= (M_x^2 + M_y^2)^{1/2} \end{aligned} \tag{3}$$

where M_m is the projection of $\mathbf{M}$ in the rotating xy plane and $M_0 = |\mathbf{M}_0| = |\mathbf{M}|$. $B_e = [(B_0-\omega/\gamma)^2 + B_1^2]^{1/2}$, $\tan\vartheta = B_1/(B_0-\omega/\gamma)$, and x is an offset parameter given as $x = (B_0-\omega/\gamma)/B_1$ with $\tan\vartheta = 1/x$, $\sin\vartheta = (1+x^2)^{-1/2}$, and $B_e = B_1(1+x^2)^{1/2}$. ϕ is

defined as a nutation angle of M_0 around B_e in time t and ϕ_0 is defined as the rotation angle of M_0 in the same duration time t around B_1, thus $\phi=\gamma B_e t$, $\phi_0=\gamma B_1 t$, and $\phi=\phi_0(1+x^2)^{1/2}$ holds. The phase angle Ω of M_m from the x axis in the xy plane is defined as $\Omega=\tan^{-1}(M_y/M_x)$ and the tipping angle α of **M** with respect to the z axis after the microwave pulse excitation is defined as $\sin\alpha=M_m/M_0=[\{\sin^2\phi + x^2(1-\cos\phi)^2/(1+x^2)\}/(1+x^2)]^{1/2}$.

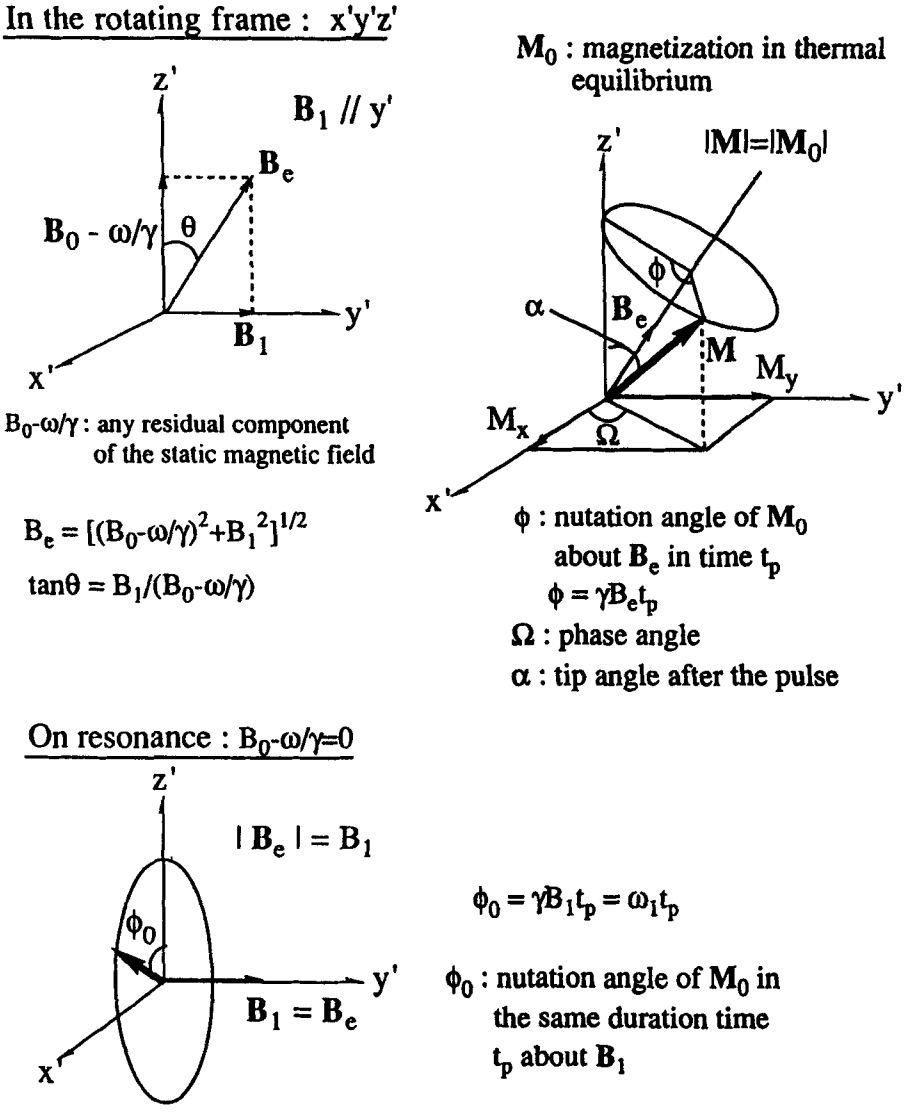

FIGURE 2 Nutation of the magnetization **M** in the rotating frame with B_1. B_1 is the microwave field pulse with a width t_p. The nutation angle ϕ of **M** is defined as the angle around the effective field B_e in time t_p.

The quantum mechanical description of an ensemble of spin systems in pulse experiments frequently invokes the equation of motion of the density matrix $|\rho(t)>$ (a ket in Liouville space) governed by the Liouville-von Neuman equation. The effect of a coherent microwave field $\mathbf{B}_1$ perpendicular to the magnetic field $\mathbf{B}_0$ beginning at t=0 is given as

$$H_1 = -\omega_1 S_y(e^{i\omega t}+e^{-i\omega t}) \tag{4}$$

with $\omega_1 = -\gamma B_1$. The equation of motion for $|\rho(t)>$ is governed by

$$d|\rho(t)>/dt = -i(\hat{H}_0+\hat{H}_1(t))|\rho(t)>, \tag{5}$$

where only the electron Zeeman term is considered, thus $H_0=-\omega_0 S_z$ and $\omega_0=-B_0/\gamma$. Transforming into the rotating frame with the frequency ω of the microwave field around the z-directon // $\mathbf{B}_0$ gives

$$d|\rho_R(t)>/dt = -i\hat{H}_R(t)|\rho_R(t)> \tag{6}$$

where $H_R(t)$ and $|\rho_R(t)>$ stand for the Hamiltonian and the density matrix defined in the rotating frame, respectively, as

$$|\rho_R(t)> = e^{-i\omega t\hat{S}z}|\rho(t)> \tag{7}$$

and

$$H_R(t) = -[\Delta\omega S_z+H_{1,R}(t)] \tag{8}$$

with

$$H_{1,R}(t) = e^{-i\omega t Sz}H_1(t)e^{i\omega t Sz} \tag{9}$$

and the resonance offset frequency $\Delta\omega$ is defined as $\Delta\omega=-(\omega-\omega_0)$. Equation (9) is rewritten as

$$H_{1,R}(t) = -\omega_1 S_y(1+\cos 2\omega t)-\omega S_x \sin 2\omega t. \tag{10}$$

The secular term $-\omega_1 S_y$ causes a rotation around the y axis with the frequency ω_1. The non-secular (time dependent) term arising from the counter-rotating part of the

microwave field does not contribute to the rotation in the first order and contributes only in higher order. The non-secular contribution called the Bloch-Siegert shift can be neglected in first order. Thus, the rotating-frame Hamiltonian is given as

$$H_R(t) = -(\Delta\omega S_z + \omega_1 S_y). \tag{11}$$

Assuming the initial density matrix $|\rho(0)\rangle = |S_z\rangle$, the solution for Equation (6) in the rotating frame is given as

$$\begin{aligned} |\rho_R(t)\rangle &= e^{it(\Delta\omega\hat{S}z + \omega_1\hat{S}y)}|\rho(0)\rangle \\ &= e^{i\vartheta\hat{S}x}\, e^{it\omega_e\hat{S}z}\, e^{-i\vartheta\hat{S}x}|S_z\rangle, \end{aligned} \tag{12}$$

where

$$\omega_e^2 = \Delta\omega^2 + \omega_1^2 \tag{13}$$

and

$$\tan\theta = \omega_1/\Delta\omega. \tag{14}$$

From Equation (12) we obtain

$$|\rho_R(t)\rangle = -\sin\vartheta\sin\omega_e t\,|S_x\rangle + \sin\vartheta\cos\vartheta(1-\cos\omega_e t)|S_y\rangle + (\cos^2\vartheta + \sin^2\vartheta\cos\omega_e t)|S_z\rangle. \tag{15}$$

Equation (15) is equivalent to Equations (1)-(3) obtained from the classical vectorial desctiption. In the case of on-resonance, i.e. $\Delta\omega = -(\omega - \omega_0) = 0$,

$$\begin{aligned} |\rho_R(t)\rangle &= e^{it\omega_1\hat{S}y}|S_z\rangle \\ &= \cos\omega_1 t\,|S_z\rangle - \sin\omega_1 t\,|S_x\rangle. \end{aligned} \tag{16}$$

Particularly, applying $\mathbf{B}_1$ for a period corresponding to a $\pi/2$-pulse transfers the initial magnetization $|\rho(0)\rangle = |S_z\rangle$ into the magnetization along the x axis, i.e. $\rho|(\pi/2\omega_1)\rangle = -|S_x\rangle$.

For the high-spin state with the spin quantum number S, the fine-structure term $H_D = \mathbf{S}\cdot\mathbf{D}\cdot\mathbf{S}$ features in the total spin Hamiltonian, where

$$H_D = \omega_D(S_Z^2 - S^2/3) + \omega_E(S_X^2 - S_Y^2) \tag{17}$$

in the principal-axis system of the fine-structure tensor **D**. For vanishing H_D or $H_D \ll H_1$ the ensemble of high spins nutates at the frequency of $\omega_1 = -\gamma B_1$ under the

on-resonance condition, where ω_1 is independent of S. For non-vanishing H_D, the nutation is modified due to the presence of H_D in the rotating frame and is not described by a single frequency. In the extreme limit of $H_D >> H_1$, however, the nutation frequency ω_n is simply expressed as

$$\omega_n = \omega_1 [S(S+1) - M_S M_S']^{1/2}, \tag{18}$$

where M_S and M_S' denote the electron spin sublevels involved in the ESR transition:[18,19] The rotating-frame matrix element corresponding to the transition is given in first order as

$$\langle S,M_S | H_{1,R} | S,M_S' \rangle = -\omega_1 [(S + M_S)(S - M_S')]^{1/2}, \tag{19}$$

where $M_S' = M_S - 1$ for the allowed ESR transitions . Thus, for $H_D >> H_1$, the nutation spectrum depends on S and M_S.[18,19] For integral spins, $S=1,2,3,\cdots$, $\omega_n = \omega_1 [S(S+1)]^{1/2}$ for the $|S,M_S=1\rangle$ -- $|S,M_S'=0\rangle$ or $|S,M_S=0\rangle$ -- $|S, M_S'=-1\rangle$ transition. Therefore, even if the EPR transitions involving the $|S,M_S=0\rangle$ level overlap due to the small ω_D values, the spin quantum number S can be discriminated in the nutation spectrum. Practically, the offset frequency effect on the nutation must be carefully considered in some cases in order to carry out magnetic-field swept nutation spectroscopy. For half-integral spins, $S=3/2, 5/2, \cdots$, the fine-structure term $\omega_D(2M_S-1)$ in first order is vanishing for the $|S,M_S=1/2\rangle$ -- $|S,M_S'=-1/2\rangle$ transition, and higher-order corrections due to the fine-structure term contribute only as off-axis extra lines in the powder-pattern fine-structure spectrum if ω_D is large.[25] The corresponding nutation frequency ω_n is given as $\omega_n = \omega_1(S+1/2)$. Thus, the nutation spectrum is distinguishable from both S=1/2 and other S's even if the fine-structure splitting does not feature in the cw ESR spectrum because of line-broadening, large ω_D values and so on. For intermediate cases, i.e. $H_D \sim H_1$, the nutation spectrum appears more or less complicated, but the spectrum can be interpretable using the rotating-frame total spin Hamiltonian.[12,13]

In addition, multiple quantum transitions can be observable in the nutation spectrum even in the extreme limit of $H_D >> H_1$. The nutation frequency arising from the multiple quantum transition is considerably reduced due to the scaling effect of the effective field which spin ensembles experience in the rotating frame, as described below. In Table I are summarized nutation frequencies ω_n on resonance for various cases of S and H_D at experimentally typical discretions.

TABLE I On-resonance nutation Frequencies for various cases.

	ω_n, ω_n^{dq}, ω_n^{tq}
$H_D = 0$	$\omega_n=\omega_1$
$H_D << H_1$	$\omega_n\sim\omega_1$
$H_D \sim H_1$	not single ω_n
$H_D >> H_1$	$\omega_n=\omega_1[S(S+1)-M_SM_S']^{1/2}$. $\omega_n=\omega_1(S+1/2)$
	$(M_S'=M_S-1)$ for the $M_S=1/2 \leftrightarrow M_S'=-1/2$ transition ($S = 3/2, 5/2, 7/2, \cdots$).
	$\omega_n=\omega_1[S(S+1)]^{1/2}$ for the $M_S=0 \leftrightarrow M_S'=-1$ or $M_S=1 \leftrightarrow M_S'=0$ transition ($S= 1, 2, 3, \cdots$).
	$\omega_n^{dq}=\omega_1(\omega_1/\omega_D)$ for $S = 1$
	$\omega_n^{dq}=\omega_1(7\omega_1/4\omega_D)$ for $S = 3/2$
	$\omega_n^{tq}=\omega_1(3\omega_1/8\omega_D)^2$ for $S = 3/2$

ω_n^{dq} and ω_n^{tq} denote the nutation frequency for double and triple quantum transitions ($S \geq 1$), respectively.

Nutation Spectrum of Multiple Quantum Transitions

The three-sublevel system is a well-established model to discuss double quantum transitions and coherence effects in spectroscopy.[26] The three-level model also has been applied to other multi-level systems, simplifying actual systems to give reasonable theoretical interpretations to a variety of transient phenomena.[27-29] Nevertheless, the nutation of multiple quantum transitions has not been fully expounded in ESR spectroscopy.

Following Vega-Pines-Wokaun-Ernst approach of the fictitious spin 1/2 operator in terms of the Zeeman basis,[30,31] we treat the S=1 spin Hamiltonian in the rotating frame to obtain a physical picture of transient nutation phenomena for double quantum transitions. The spin Hamiltonian for an S=1 system is

$$H_0= -\omega_0S_Z + \omega_D[S_Z^2-S(S+1)/3] + \omega_E(S_X^2-S_Y^2). \quad (20)$$

For simplicity, we will neglect the third term hereafter. The single quantum ESR transitions appear at $\omega_0\pm\omega_D$ and the double quantum transition appears at ω_0. Introducing fictitious spin 1/2 operators in terms of the Zeeman basis, the total spin

operators in Equation (20) are expressed as

$$\left.\begin{aligned} S_k &= \sqrt{2}\,(S_k^{1-2} + S_k^{2-3}) \qquad (k=x,y) \\ S_z &= 2(S_z^{1-2} + S_z^{2-3}) = 2S_z^{1-3}, \end{aligned}\right\} \quad (21)$$

where S_l^{1-2} and S_l^{2-3} (l=x,y,z) are single quantum operators, and S_l^{1-3} (l=x,y,z) is a double quantum operator. Other bilinear combinations of total spin operators appearing in Equation (20) can be generally expressed by linear combinations of fictitious spin 1/2 operators. Thus, the spin Hamiltonian of Equation (20) can be rewritten in terms of the fictitious spin 1/2 operator as

$$H_0 = -2\omega_0 S_z^{1-3} + (2\omega_D/3)(S_z^{1-2} - S_z^{2-3}) \quad (22)$$

and similarly, the secular part of the microwave field Hamiltonian is given as

$$H_1 = -\omega_1 S_k = -\sqrt{2}\,\omega_1(S_k^{1-2} + S_k^{2-3}), \qquad (k=x,y) \quad (23)$$

Thus, the total spin Hamiltonian H_R in the rotating frame is written in terms of the fictitious spin 1/2 operator as

$$H_R = -2(\omega_0-\omega)S_z^{1-3} + (2\omega_D/3)(S_z^{1-2} - S_z^{2-3}) - \sqrt{2}\,\omega_1(S_k^{1-2} + S_k^{2-3}). \quad (24)$$

Now, for simplicity we first treat the single quantum transition and next the double quantum transition for an S=1 system with the offset frequency effect taken into account. The two single quantum transitions appear at $\omega=\omega_0\pm\omega_D$. First, let us consider the 2-3 transition. Defining $\Delta\omega=\omega_0+\omega_D-\omega$ with $\Delta\omega<<\omega_D$ makes us rewrite Equation (22) as

$$H_{0,R} = -\Delta\omega S_z^{2-3} + (4\omega_D/3 - \Delta\omega)(S_z^{1-2} + S_z^{1-3}), \quad (25)$$

where the triangular relation for the z-component of the fictitious spin 1/2 operator $S_z^{1-2} + S_z^{2-3} + S_z^{1-3} = 0$ and the similar relation under cyclic pemutation with respect to 1,2 and 3, and $S_z^{3-1} = S_z^{1-3}$ are used. The eigenvalues $E_0^{R_i}$ (i=1,2,3) in the rotating frame are given as

$$\left.\begin{aligned} E_0{}^{R}{}_1 &= 4\omega_D/3 - \Delta\omega \\ E_0{}^{R}{}_2 &= -2\omega_D/3 \\ E_0{}^{R}{}_3 &= -2\omega_D/3 + \Delta\omega. \end{aligned}\right\} \quad (26)$$

In the extreme limit of $H_D >> H_1$, i.e. $\omega_D >> \omega_1$, the term $\sqrt{2}\omega_1 S_k{}^{1-2}$ in Equation (24) can be neglected since it couples 1 and 2 levels separated by $2\omega_D$. Thus, the total spin Hamiltonian in the rotating frame H_R is truncated to

$$H_R = H_R{}^{2-3} + H_R{}^{1-2,1-3}, \quad (27)$$

where

$$H_R{}^{2-3} = -\Delta\omega S_z{}^{2-3} - \sqrt{2}\omega_1 S_k{}^{2-3}, \quad (28)$$

$$H_R{}^{1-2,1-3} = (4\omega_D/3 - \Delta\omega)(S_z{}^{1-2} + S_z{}^{1-3}), \quad (29)$$

and $[H_R{}^{2-3}, H_R{}^{1-2,1-3}] = 0$. Here, we arrive at a physical picture for the 2-3 transition, which is described by $H_R{}^{2-3}$. The S=1 spin nutates around an effective field with a frequency $\omega_e = (\Delta\omega^2 + 2\omega_1{}^2)^{1/2}$ which is tilted by an angle of $\vartheta = \tan^{-1}(\sqrt{2}\omega_1/\Delta\omega)$ with respect to the z-axis. If microwave excitation is carried out on-resonance for the 2-3 transition, i.e $\Delta\omega = 0$, the spin precesses at the nutation frequency $\omega_n = \omega_e = \sqrt{2}\omega_1$, as given in the preceding section: $\omega_n = [S(S+1)]^{1/2}\omega_1$ (S=1). The on-resonance nutation is given as

$$\exp(i\sqrt{2}\omega_1 t S_y{}^{2-3}) S_z{}^{2-3} \exp(-i\sqrt{2}\omega_1 t S_y{}^{2-3}) = S_z{}^{2-3}\cos(\sqrt{2}\omega_1 t) - S_x{}^{2-3}\sin(\sqrt{2}\omega_1 t), \quad (30)$$

where $\rho^{2-3}(0) = S_z{}^{2-3}$ is assumed. Corresponding arguments in terms of the density matrix hold.

Now we treat the nutation of the 1-3 double quantum transition appearing at ω_0 for the S=1 system. Again we define $\Delta\omega = -(\omega - \omega_0)$ with $\Delta\omega << \omega_D$. The rotating-frame total spin Hamiltonian is given as

$$H_R = -2\Delta\omega S_z{}^{1-3} + (2\omega_D/3)(S_z{}^{1-2} - S_z{}^{2-3}) - \sqrt{2}\omega_1(S_k{}^{1-2} + S_k{}^{2-3}). \quad (31)$$

H_R can be rewritten by unitary transformations as

$$\begin{aligned} H_R{}^{U} = {} & -2\Delta\omega\cos(\vartheta/2) S_z{}^{1-3} + (1/2)(\omega_e - \omega_D) S_k{}^{1-3} \\ & + [2\omega_D/3 + (1/2)(\omega_e - \omega_D)](S_z{}^{1-2} - S_z{}^{2-3}) - \sqrt{2}\Delta\omega\sin(\vartheta/2)(S_k{}^{1-2} - S_k{}^{2-3}) \end{aligned} \quad (32)$$

with $\sin\vartheta=2\omega_1/\omega_e$, $\cos\vartheta=\omega_D/\omega_e$, and $\omega_e=[\omega_D+4\omega_1]^{1/2}$. In the extreme limit of $H_D>>H_1$, i.e. $\omega_D>>\omega_1$, we obtain

$$H_R^U = H_R^{U,1-3} + H_R^{U,1-2,2-3}, \tag{33}$$

where

$$H_R^{U,1-3} = -2\Delta\omega S_z^{1-3} + (\omega_1^2/\omega_D)S_k^{1-3} \tag{34}$$

and

$$H_R^{U,1-2,2-3} = [2\omega_D/3 + (\omega_1^2/\omega_D)](S_z^{1-2} - S_z^{2-3}), \tag{35}$$

noting $[H_R^{U,1-3}, H_R^{U,1-2,2-3}]=0$. Any action on the 1-3 double quantum transition is described by $H_R^{U,1-3}$. The S=1 spin system nutates around an effective field with $\omega_e=[4\Delta\omega^2 + (\omega_1^2/\omega_D)^2]^{1/2}$ and a tilting angle $\vartheta=\tan^{-1}[-\omega_1^2/(2\omega_D\Delta\omega)]$. If microwave excitation is carried out on-resonance for the 1-3 transition, the nutation frequency is given as $\omega_n=\omega_e=\omega_1(\omega_1/\omega_D)$, showing that $\omega_n\sim0$ is obtained due to the scaling factor $\omega_1/\omega_D<<1$.

Corresponding treatment can be applied to an S=3/2 system for the two double quantum transitions appearing at $\omega_0\pm\omega_D$ and corresponding nutation frequency ω_n undergoes a scaled field $\omega_1(7\omega_1/4\omega_D)=\omega_n$,[30b,32] giving $\omega_n<<\omega_1$ in the extreme limit of $H_1<<H_D$, i,e. $\omega_1<<\omega_D$. For a triple quantum transition appearing at ω_0 for the S=3/2 system, the corresponding nutation is induced by an effective field $B_e=-\gamma\omega_e$, i.e., $\omega_n=\omega_e=\omega_1(3\omega_1^2/8\omega_D^2)$,[32] showing that the scaling factor for the nutation frequency is $3\omega_1^2/8\omega_D^2$.

The above arguments predict that if nutation components near zero frequency are discriminated due to multiple quantum transitions and the frequency shifts as a function of the microwave amplitude are measured, the fine-structure constant ω_D can be evaluated from the nutation experiment under the assumption of $H_D>>H_1$. The nutation spectrum of multiple quantum transitions can be a measure for small ω_D values which are undetectable by conventional cw ESR spectroscopy. Since the multiple quantum nutation is intrinsic to multi-level systems ($S\geq1$), it can be used for discriminating high spins from S=1/2. The Vega-Pines-Wokaun-Ernst approach can be extended to transient nutation phenomena of arbitrary spins and more general cases, and useful experimental aspects can be predicted.[33]

EXPERIMENTAL METHOD

The nutation experiment can be made by either observing the FID or electron spin (or rotary) echo (ESE) signal $s(t_1, t_2)$ as time-domain spectroscopy (time axis t_2) by incrementing the time interval t_1 of microwave pulse excitation parametrically. The two time variables t_1 and t_2 are independent. $s(t_1, t_2)$ measured as a function of t_1 and t_2 is converted into a 1D or 2D frequency domain spectrum, i.e.,

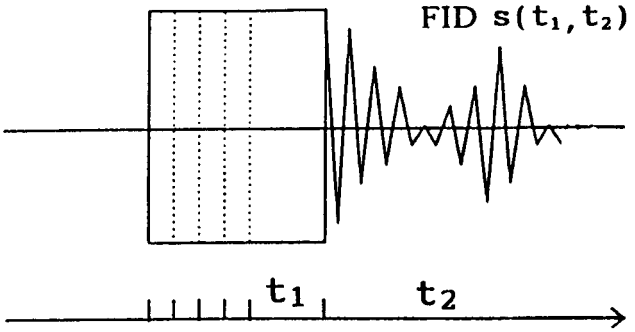

FIGURE 3 Schematic timing diagram for the FID-detected transient nutation experiment.[6] The FID signal s(t1, t2) is measured as a function of the time width t1 of the microwave pulse and is converted into a frequency-domain spectrum S(f1,t2) (or $S(t_1,f_2)$) or $S(f_1,f_2)$ by a 1D or 2D Fourier transformation, respectively.

$S(f_1, t_2)$ (or $S(t_1, f_2)$) or $S(f_1,f_2)$ by Fourier transformation. Our nutation experiment was carried out by the FID-detected method. The ESE-detected method applied to high-spin systems which undergo inhomogeneous line-broadening will be published elsewhere. The timing diagram for our nutaion experiment is schematically shown in Figure 3.[6] A current Bruker, Inc. ESP300E/380 2D FT ESR spectrometer equipped with a dielectric cavity of tunable Q_u=100~5000 was used for our nutation experiment[34] and cryogenic temperature was controlled with an Oxford helium gas-flow variable-temperature system. The microwave pulse was amplified by a 1KW pulsed traveling wave tube (TWT) amplifier. Electron spin transient nutation experiments are sensitive to a B_1 homogeneity and the B_1 gradient effect must be taken into account in the experimental interpretation,[6] but the gradient effect across the sample was not considered in our interpretation since only a small portion inside the cavity was filled with our samples. The molecular structure of a quasi 1D organic magnetic polymer A employed in our nutation experiment is depicted in Figure 1. The polymer as models for quasi 1D organic ferromagnets was elaborately designed[24] based on through-bond approach to high T_c organic ferro-

magnets.[20] The sample preparation of the polymer will be published elsewhere.[24] Mn^{2+}- and Cr^{3+}-doped powder samples were prepared by the usual methods.

RESULTS AND DISCUSSION

Inorganic High-Spin Systems: Mn^{2+}- and Cr^{3+}-Doped MgO Powder

Figures 4 and 5 show a cw ESR spectrum and a typical nutation spectrum of the $^{55}Mn^{2+}$(S=5/2, I=5/2)-doped MgO powder observed at ambient temperature, respectively. The cw spectrum is comprised of the six hyperfine allowed ($\Delta M_I=0$) transitions belonging to the $|S,M_S=1/2\rangle$ --- $|S,M_S'=-1/2\rangle$ fine-structure transition. All the six lines gave the same nutation frequency $\omega_n=12.24$ MHz at the microwave amplitude of 20db (the corresponding absolute microwave power at the sample site has not been known yet), showing that the six lines are attributable to the ESR transition involving the same electron spin sublevels and the same ΔM_I selection rule. The observed frequency ω_n agreed with three times of $\omega_1=\omega_n(S=1/2)$ observed for a reference standard (a single crystal of DPPH), demonstrating that the particular relationship $\omega_n=(S+1/2)\omega_1$ in the extreme limit of $H_D>>H_1$ holds, i.e. $\omega_n=3\omega_1$ as expected for S=5/2. Thus, the six hyperfine lines are identified to arise from the $|S=5/2, M_S=1/2\rangle$ --- $|S=5/2, M_S'=-1/2\rangle$ transition. Since the hyperfine splitting (A=0.008111 cm^{-1}) is much greater than the fine structure splitting (a'= 0.001901 cm^{-1}), the angular anomaly due to the higher-order contribution of the fine-structure term does not show up for the $|S, M_S=1/2\rangle$ --- $|S, M_S'=-1/2\rangle$ transition, this particular $|\Delta M_S|=1$ transition is apparently intensified even in the powder-pattern fine-structure spectrum of the ground state ($^6S_{5/2}$) of $^{55}Mn^{2+}$ in MgO, where the parameters A and a' refer to the isotropic hyperfine coupling constant and the additional higher-order fine-structure constant defined as

$$H_C= (a'/120)[35S_Z^4 - 30S(S+1)S_Z^2 + 25S_Z^2 - 6S(S+1) + 3S^2(S+1)^2] + (a'/48)(S_+^4 + S_-^4) \quad (36)$$

with $a'=\beta_C/6$ and β_C refers to the octahedral constant. For S=5/2, Equation (36) reduces to

$$H_C= (a'/384)(112S_Z^4 - 760S_Z^2 + 567) + (a'/48)(S_+^4 + S_-^4), \quad (37)$$

which is comprised of the octahedral crystal-field operators connecting spin sublevels with M_S values differing by ± 4.[35,36]

Cr^{3+} and its complexes among the $3d^3$ ions have been extensively studied.

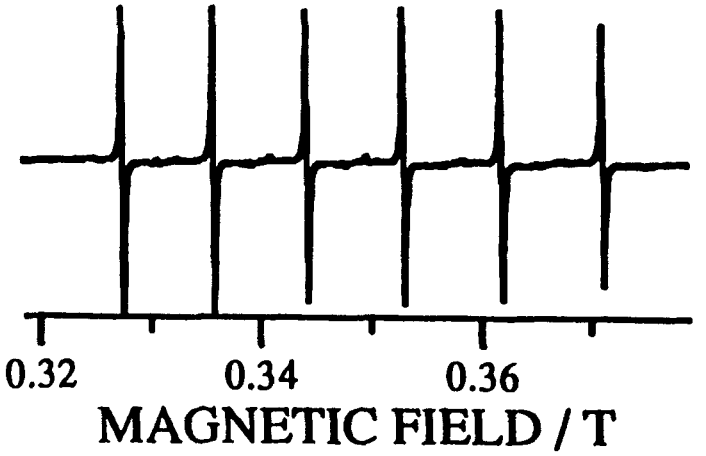

FIGURE 4 Cw ESR spectrum of Mn^{2+}(S=5/2, I=5/2)-doped MgO powder observed at ambient temperature. The six absorption lines arise from the hyperfine allowed transitions ($\Delta M_I=0$) belonging to the $|S, M_S=1/2\rangle$ --- $|S,M_S'=-1/2\rangle$.

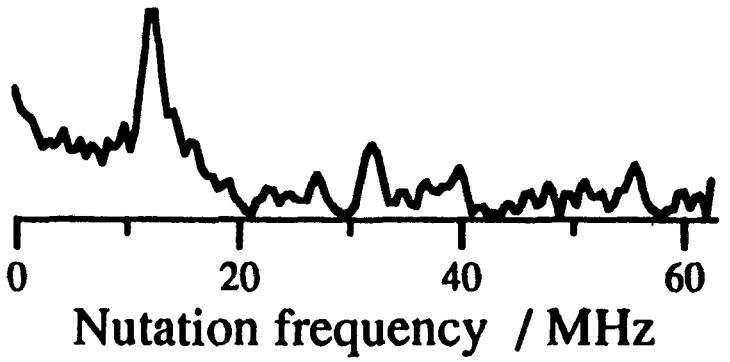

FIGURE 5 Nutation spectrum of $^{55}Mn^{2+}$(S=5/2, I=5/2)-doped MgO powder observed at ambient temperature. The hyperfine transition at 0.3357T was monitored for the measurement of the transient nutation (microwave amplitude: 20db). The absolute power level of microwave was not calibrated.

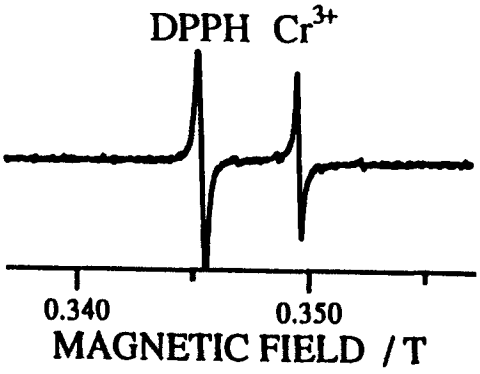

FIGURE 6 Cw ESR spectrum of Cr^{3+} (S=3/2)-doped MgO powder observed at ambient temperature. The signal appearing on the lower field side arises from a DPPH single crystal as the reference standard.

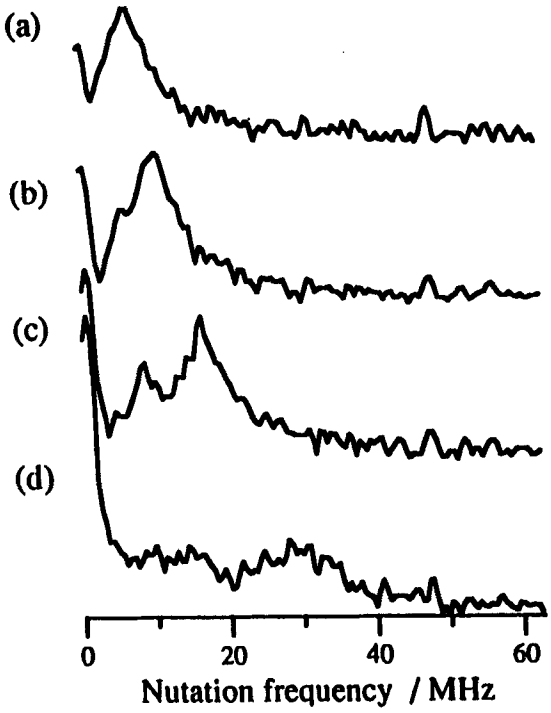

FIGURE 7 Nutation spectra of Cr^{3+} (S=3/2)-doped MgO powder observed at ambient temperature. The nutation was measured on the central line of $^{50,52,54}Cr^{3+}$: (a) - (d) show the dependence of the nutation on microwave excitation amplitude:(a)25db (b)20db (c)15db (d)10db. The power levels are given only for relative comparison, but they were linear.

Figure 6 shows a typical ESR spectrm of Cr^{3+} in octahedral symmetry in MgO powder and the signal from the reference standard of DPPH. It has been well-documented that the Cr^{3+} spectrum is isotropic with g= 1.9796 and the vanishing fine-structure term at ambient temperature and the central line arises from $^{50,52,54}Cr^{3+}$ (I=0) and the hyperfine quartet satellite lines are due to $^{53}Cr^{3+}$(I=3/2, natural abundance 9.54%) with A=0.00163 cm^{-1}.[37] Figures 7(a)-(d) show nutation spectra obtained from the central line of Cr^{3+} in MgO powder at ambient temperature at various microwave amplitude levels. In Figure 7(d) two nutation frequencies are seen near 15 (ω_1) and 30 MHz ($2\omega_1$). The nutation frequency component at ω_1(15 MHz at 10db) coincided with $\omega_n(S=1/2)=\omega_1$ of the reference standard in the whole range of the microwave excitation power level. With diminishing microwave amplitude, the $2\omega_1$ peak approached the ω_1 peak, as seen from Figure 7(d) to 7(a), and coincided with the ω_1 peak at weak levels of the microwave amplitude. The nutation spectra shown in Figure 7(d)-(b) can be classified in the intermediate regime $H_D \sim H_1$, since the $2\omega_1$ frequency corresponds to $\omega_n(S=3/2)=(3/2+1/2)\omega_1$ in the extreme limit of $H_D >> H_1$, identifying the nutation frequency $\omega_n(S)=2\omega_1$ to arise from the $|S, M_S=1/2\rangle$ --- $|S, M_S'=-1/2\rangle$ ESR transition (S=3/2). As described in the preceding theoretical treatment, the vanishing H_D does not produce any single-quantum nutation frequency different from ω_1. Thus, the present nutation experiment shows that Cr^{3+} in MgO is located in lower symmetric enviroments than octahedral symmetry. Conventional cw ESR spectroscopy has never detected such symmetry reduction due to a distortion taking place at the impurity lattice site in MgO. Isoya et al. is the first who have found such a subtle distortion responsible for non-vanishing fine-structure terms with the help of the electron spin transient nutation technique.[18]

It is interesting to note a behavior of the nutation frequency near $\omega_n \sim 0$ in Figure 7. Microwave amplitude dependence of the nutation frequency, i.e. an appreciable higher-frequency shift and enhanced intensity near $\omega_n \sim 0$ with increasing the amplitude, suggests the occurrence of double quantum transitions for the high-spin system with a small ω_D value in the extreme limit of $H_D >> H_1$. According to the the theoretical prediction described in the second section, the two double quantum transitions occur for an S=3/2 system with the microwave field $\mathbf{B}_1$, i.e. ω_1 ($B_1=-\gamma\omega_1$) scaled by $7\omega_1/4\omega_D$, showing that the nutation arising from the double quantum transition appears near $\omega_n \sim 0$ in the extreme limit of $H_1 << H_D$ and that ω_n departs from nearby zero frequency with increasing microwave amplitude, i.e. ω_1. Thus, the theoretical prediction can qualitatively interpret the observed behavior of the

nutation spectrum of the nearby zero frequency. Also, the possible occurrence of the contribution from a triple quantum transition appearing at the central ESR line ω_0 can not be excluded. For the triple quantum transition of S=3/2 systems the scaling factor is $3\omega_1^2/8\omega_D^2$, as given in Table I and the triple quantum nutation appears at $\omega_n \sim 0$ in the extreme limit of $H_1 << H_D$.

A Quasi 1D Organic High-Spin Polymer A

Figure 8 shows a cw ESR spectrum of the solid-state polymer A observed at 6.7K. The ESR line shape was Lorentzian, indicating the exchange-narrowing taking place in the system. Figures 9(a) and (b) show the microwave amplitude dependence of the on-resonance nutation spectra of the polymer A where the FID signal $s(t_1, t_2)$ was measured at 6.7K. Figure 10 shows a 2D representation of the 1D Fourier-transformed FID signal $s(t_1, t_2)$ as a function of the time-domain nutation defined by the time-axis t_1 segmentation, noting that the FID signal $s(t_1, t_2)$ was Fourier-transformed only along the time-axis t_2 into the frequency-domain power spectra. The FID signal $s(t_1, t_2)$ was obtained at good signal-to-noise ratios by incrementing the interval t_1, as seen in Figure 10. In Figure 9 many nutation-frequency components depending on the microwave amplitude are seen. They were reproducible and were not distinguishable at elevated temperatures. In the extreme limit of $H_D >> H_1$ the lowest distinguishable nutation peak $\omega_n(S_i)$ besides the strong one near zero frequency corresponds to an effective spin quantum number $S_i > 2$, which was evaluated by comparison with the nutation frequency $\omega_n(S=1/2)$ of the reference standard (a single crystal of DPPH): $\omega_n(S_i) > 2\omega_n(S=1/2)$. Table II shows the peak assignments to effective spin quantum numbers assuming that $M_S = 0 \leftrightarrow M_S' = \pm 1$ transitions are dominant in the nutation spectra. The nutation experiment on the polymer A clearly identified the polymer A in the solid state to be a mixture of high-spin assemblages with various spin quantum numbers S_i's some of which exceed two. This finding supports the experimental result from the magnetization curve fitting for the same polymer: the Brillouin function fitting gave an effective S=2.[24] The magnetization curve fitting is insensitive to an ensemble of various spin quantum numbers S's. This fitting procedure is problematic and impractical with the increasing number of S's expected for extended spin structures of magnetic polymers or spin clusters. The present nutation experiment demonstrates that electron spin transient nutation techniques are more suitable for the spectroscopic discrimination of S's for high-spin assemblages, noticing that one of the drawbacks of the nutation method is time resolution. For further systematic identification of S's the sample preparation and nutation experiments of high-spin oligomers A with

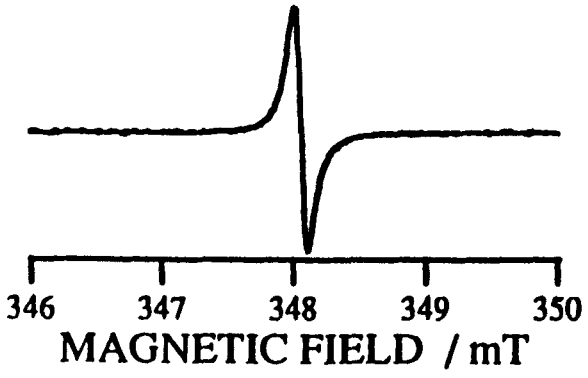

FIGURE 8 Cw ESR spectrum of a quasi 1D organic high-spin polymer A in the solid state observed at 6.7K.

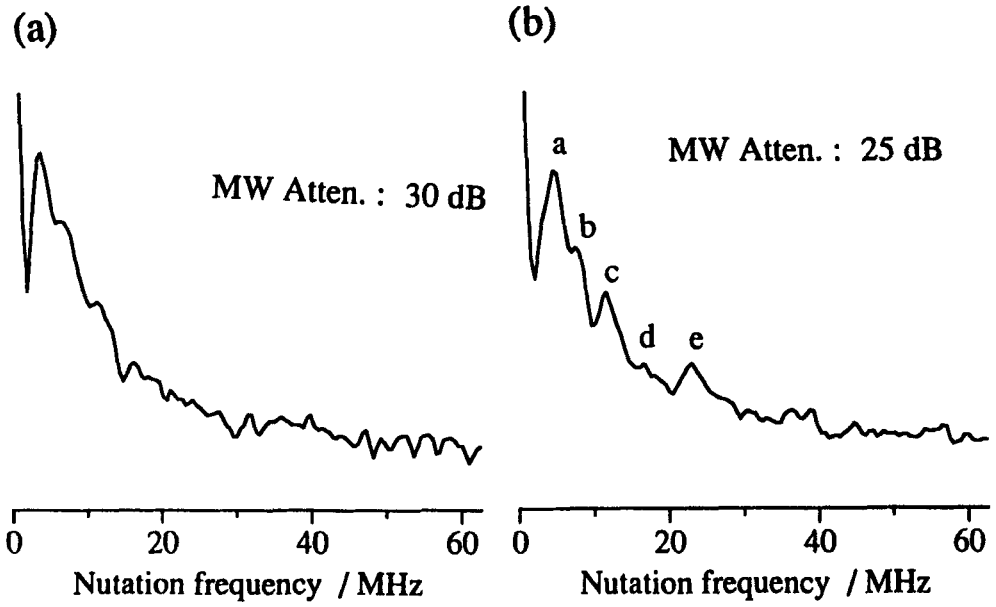

FIGURE 9 Nutation spectra of a solid-state polymer A observed at 6.7K. The microwave amplitude dependence of the on-resonance nutation is shown: (a)30db (b)25db: The corresponding absolute microwave power was not calibrated.

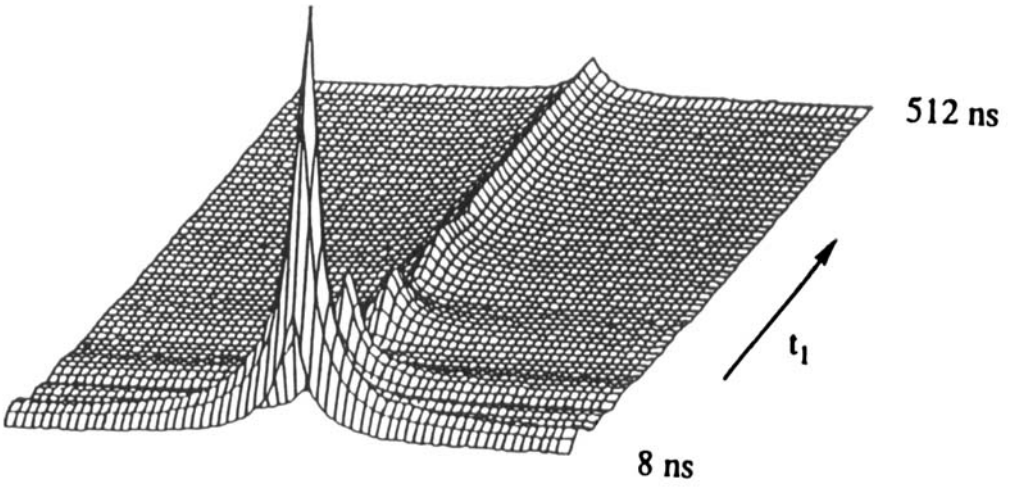

FIGURE 10 2D representation of the 1D Fourier-transformed FID signal $s(t_1, t_2)$ of a solid-state polymer A as a function of the time-domain nutation defined by the time axis t_1. The FID signal $s(t_1, t_2)$ was Fourier transformed only along the time-axis t_2 into the frequency-domain power spectra.

TABLE II The nutation peak assignments to effective spin quantum numbers appearing in the nutation spectra observed from the quasi-1D polymer A at 6.7 K.

	ω_n	ω_n/ω_1	S	$[S(S+1)]^{1/2}$
a	4.84 (= ω_1)	1	1/2	
b	7.88	1.63	1	$[1(1+1)]^{1/2} = 1.41$
c	11.47	2.37	2	$[2(2+1)]^{1/2} = 2.45$
d	16.73	3.45	3	$[3(3+1)]^{1/2} = 3.46$
e	22.95	4.74	4	$[4(4+1)]^{1/2} = 4.47$

S=1 or 3/2 are under way. The effective spin multiplicities of molecular high-spin components in the solid-state polymer A can be hampered by both inter- and intramolecular antiferromagnetic couplings and the structural disconnection or termination of the topologically controlled π spin network. The present spectroscopic evidence of the occurrence of molecular high-spin components, however, illustrates that the molecular design controlling the topological spin polarization is workable for constructing π-conjugated organic super high-spin/magnetic polymers.

CONCLUSIONS

The FID-detected electron spin transient nutation spectroscopy was applied to MgO powder samples doped with Mn^{2+}(S=5/2) and Cr^{3+}(S=3/2) in their high-spin ground state, demonstrating the advantages inherent in the nutation spectroscopy. The nutation experiment in the extreme limit of $H_D >> H_1$ (weak microwave excitation limit) can identify the ESR transition. A non-vanishing H_D due to a slight departure from octahedral symmetry was detected at ambient temperature for Cr^{3+} in MgO powder. This finding contrasts with the well-documented fact that the electronic ground state of Cr^{3+} in MgO is characteristic of the vanishing fine-structure term in the spin Hamiltonian. The nutation spectrum appearing at $\omega_n \sim 0$ indicates the possible occurrence of multiple quantum transitions for an S=3/2 system. A particular spectroscopic feature associated with the double or triple quantum transition was qualitatively interpretable by the theoretical consideration in the extreme limit of $H_D >> H_1$.

The nutation method was for the first time applied to a quasi 1D high-spin organic polymer as one of the most complex amorphous spin assemblages, identifying that the polymer with an exchange-narrowing ESR lineshape is comprised of high-spin assemblages with effective molecular spin quantum numbers S's greater than two. It can be concluded that electron spin transient nutation spectroscopy is a simple and useful method for the identification of spin quantum numbers and ESR transitions even for the cases of apparently vanishing fine-structure splittings and the method is applicable to spin systems with residual fine-structure terms in the spin Hamiltonian. Fundamental bases for electron spin transient nutation were also described, particularly for S=1 and 3/2, in the extreme limit of $H_D >> H_1$, emphasizing a view point of nutation spectroscopy.

ACKNOWLEDGMENTS

This work has been supported by a Grand-in-Aid for Scientific Research on Priority Area "Molecular Magnetism" (Area No.228/04 242 103, 04 242 104 and 04 242 105) from the Ministry of Education, Culture and Science, Japan and also by the Ministry of International Trade and Industries (NEDO Project). One of the authors (T.T.) is grateful to Professor A. Schweiger (E.T.H., Zürich) and Professor J. Isoya (Univ. of Library and Information science, Tsukuba) for their stimulating suggestions.

REFERENCES

1. T. Ichikawa, *Bunseki*, No.12, 890(1982).
2. J. Isoya, *Bunseki*, No.4, 229(1988).
3. A. Schweiger, *Angew. Chem. Int. Ed. Engl.*, **30**, 265(1991).
4. C. P. Keijzers, E. J. Reijerse, and J. Schmidt (eds.), *Pulsed EPR: A new field of applications* (North Holland, Amsterdam/Oxford/New York/Tokyo, 1989).
5. A. J. Hoff (ed.), *Advanced EPR, Applidcations in biology and biochemistry* (Elsevier, Amsterdam/Oxford/New York/Tokyo, 1989).
6. L. Kevan and M. K. Bowman (eds), *Modern Pulsed and Continuous-wave Electron Spin Resonance* (John Wiley and Sons, New York/Chichester/Brisbane/ Toronto/Singapore, 1990).
7. S. A. Dikanov and Y. D. Tsvetkov, *Electron Spin Echo Envelope Modulation (ESEEM) Spectroscopy* (CRC Press, Bocan Raton/Ann Arbor/London/Tokyo, 1992)
8. H. C. Torrey, *Phys. Rev.*, **76**, 1059(1949).
9. I. Solomon, *Phys. Rev. Lett*, **2**, 301(1959).
10. C. S. Yannoni and R. D. Kendrick, *J. Chem. Phys.*, **74**, 747(1981).
11. a) A. Samoson and E. Lippmaa, *Chem. Phys, Lett.*, **100**, 205(1983).
    b) A. Samoson and E. Lippmaa, *Phys. Rev.* **B28**, 6567(1983).
12. F. M. M. Geruts, A. P. M. Kenthens, and W. S. Veeman, *Chem. Phys. Lett.*, **120**, 206 (1985).
13. A .P. M. Kenthens, J. J. M. Lemmens, F. M. M. Geruts, and W. S. Veeman, *J. Magn. Reson.*, **71**, 62(1987).
14. a) R. Janssen, G. A. H. Tijink, and W. S. Veeman, *J. Chem. Phys.*, **88**, 518(1988).
    b) R. Janssen and W.S. Veeman, *J. Chem. Soc. Faraday Trans.*, **84**, 3747(1988).
15. S. S. Kim and S. I. Weissman, *Rev. Chem. Intermed.*, **3**, 107(1980).
16. R. Furrer, F. Fujara, C. Lange, D. Stehlik, H. M. Vieth, and W. Vollman, *Chem. Phys. Lett.*, **75**, 332(1980).
17. D. Stehlik, C. H. Bock, and M. C. Thurnauer, *Advanced EPR*, ed. A. J. Hoff (Elsevier, Amsterdam/Oxford/New York/Tokyo, 1989). P.371.
18. J. Isoya, H. Kanda, J. R. Norris, J. Tang, and M. K. Bowman, *Phys. Rev.*, **B41**, 3905(1990).
19. A. V. Astaskin and A. Schweiger, *Chem. Phys. Lett.*, **174**, 595(1990).
20. a) K. Itoh, *Chem. Phys. Lett.*, **1**, 235(1967).
    b) E. Wasserman, R. W. Murray, W. A. Yager, A. M. Trozzolo, and G. Smolinsky, *J. Am. Chem. Soc.*, **89**, 5076(1967).
    c) S. Morimoto, F. Tanaka, K. Itoh, and N. Mataga, *Preprints of Symposium on Molecular Structure* (Chem. Soc. Japan), 67(1968).

d) N. Mataga, *Theor. Chim. Avta*, **10**, 372(1968).
e) K. Itoh, *Bussei*, **12**, 635(1971).
f) K. Itoh, *Pure & Appl. Chem.*, **50**, 1251(1978).
g) A. A. Ovchinnikov, *Theor. Chim. Acta*, **47**, 297(1978).
h) T. Takui and K. Itoh, *J. Materials Sci. Soc. Japan*, **28**, 315(1991) and references therein.
21. a) H. M. McConnell, *J. Chem. Phys.*, **39**, 1910(1963).
b) H. M. McConnell, *Proc. R. A. Welch Found. Chem. Res.*, **11**, 144(1967).
22. a) J. S. Miller, A. J. Epstein, and W. M. Reiff, *Chem. Rev.*, **88**, 201(1988) and references therein.
b) J. S. Miller, A. J. Epstein, and W. M. Reiff, *Acc. Chem. Res.*, **22**, 114(1988) and references therein.
23. For a recent overview, see the following references.
a) J. S. Miller and D. A. Dougherty (eds.), *Mol. Cryst. Liq. Cryst.*, **176**, 1-562(1989).
b) L. Y. Chang, P. M. Chaikin, and D. O. Cowan (eds.), *Advanced Organic Solid State Materials* (MRS, 1990) p.1-92.
c) D. Gatteschi, O. Kahn, J. S. Miller, and F. Palacio (eds.), *Molecular Magnetic Materials* (Kluwer Academic Press, 1990).
d) H. Iwamura and J. S. Miller (eds.), *Mol. Cryst. Liq. Cryst.*, **232/233** , 1-724(1993).
24. T. Kaneko, E. Tsuchida, H. Nishide and K. Yamaguchi, *J. Am. Chem. Soc.*, to be published.
25. Y. Teki, T. Takui, and K. Itoh, *J. Chem. Phys.*, **88**, 6134(1988).
26. R. G. Brewer and E. L. Hahn, *Phys. Rev.*, **All**, 1641(1975).
27. N. M. T. Loy, *Phys. Rev. Lett.*, **36**, 5624(1977).
28. H. Hatanaka, T. Terao, and T. Hashi, *J. Phys. Soc. Japan*, **39**, 835(1975).
29. H. Hatanaka and T. Hashi, *J. Phys. Soc. Lapan*, **39**, 1139(1975).
30. a) S. Vega and A. Pines, *J. Chem. Phys.*, **66**, 5624(1977).
b) S. Vega, *J. Chem. Phys.*, **68**, 5518(1978).
31. A. Wokaun and R. R. Ernst, *J. Chem. Phys.*, **67**, 1752(1977).
32. S. Vega and Y. Naor, *J. Chem. Phys.*, **75**, 75(1981).
33. K. Sato, D. Shiomi, T. Takui, and K. Itoh, to be published.
34.a) K. Holczer, D. Schmalbein, and P. Barker, *Bruker Rep.*, 7, 4(1988).
b) H. Barth, P. Höfer, and K. Holczer, *Bruker Rep.*, 2, 28(1988).
35. G. R. Hertel and H. M. Clark, *J. Phys. Chem.*, **65**, 1930(1961).
36. M. T. Hutchings, *Solid State Phys.*, **16**, 227(1964).
37. W. Low and E. L. Offenbacher, *Solid State Physics*, ed F. Seitz and D. Turnbull (Acadenic Press, New York 1965) vol. 17, p. 135.